

Gamma-Ray Bursts

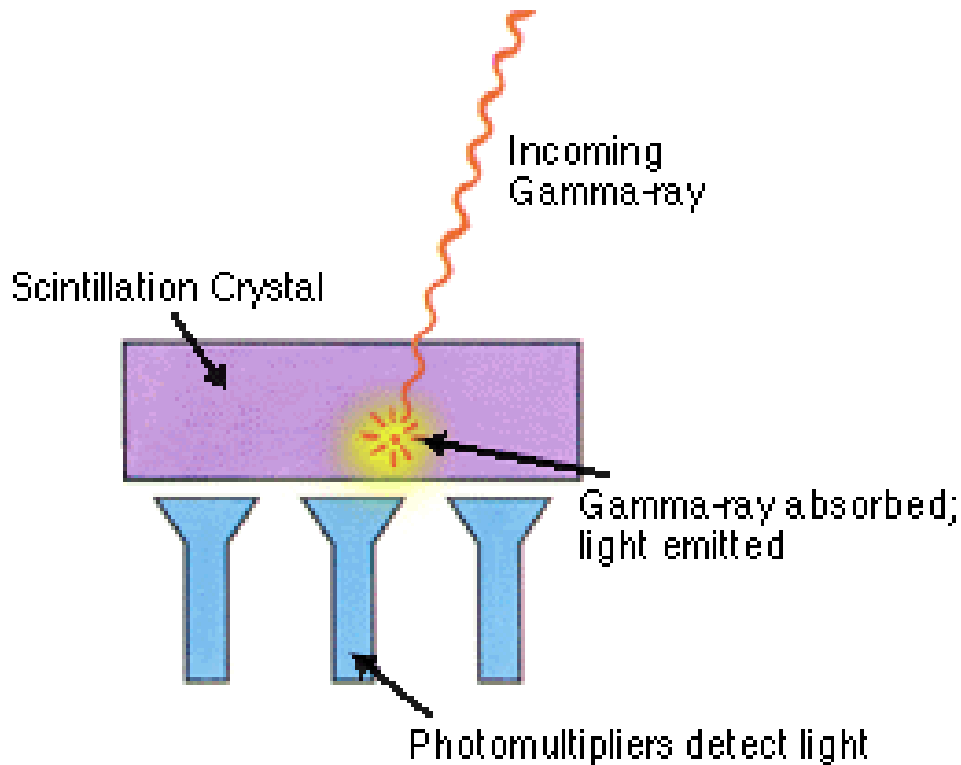
- Detectors for 20 keV to 10 MeV
- Discovery
- The early years
- BATSE
- Fast versus slow bursts
- Uniformity and $\log N - \log S$ relation
- BeppoSAX and discovery of afterglows
- Redshift measurements
- Connection of long GRBs to supernovae

Detectors for 20 keV – 10 MeV

- Can not use detectors for standard X-ray band (0.1-10 keV) because interaction cross-sections are too small – need more material.
- Thick semiconductor detectors
 - CdTe, CdZnTe, Ge, PbI₂, HgI₂, ...
 - Work like X-ray semiconductor detectors
 - Typically have pixilated readout, one channel per pixel
 - Typical thickness 0.1 to several millimeters

Detectors for 20 keV – 10 MeV

- Scintillators – convert gamma-ray to optical photons then detect optical photons

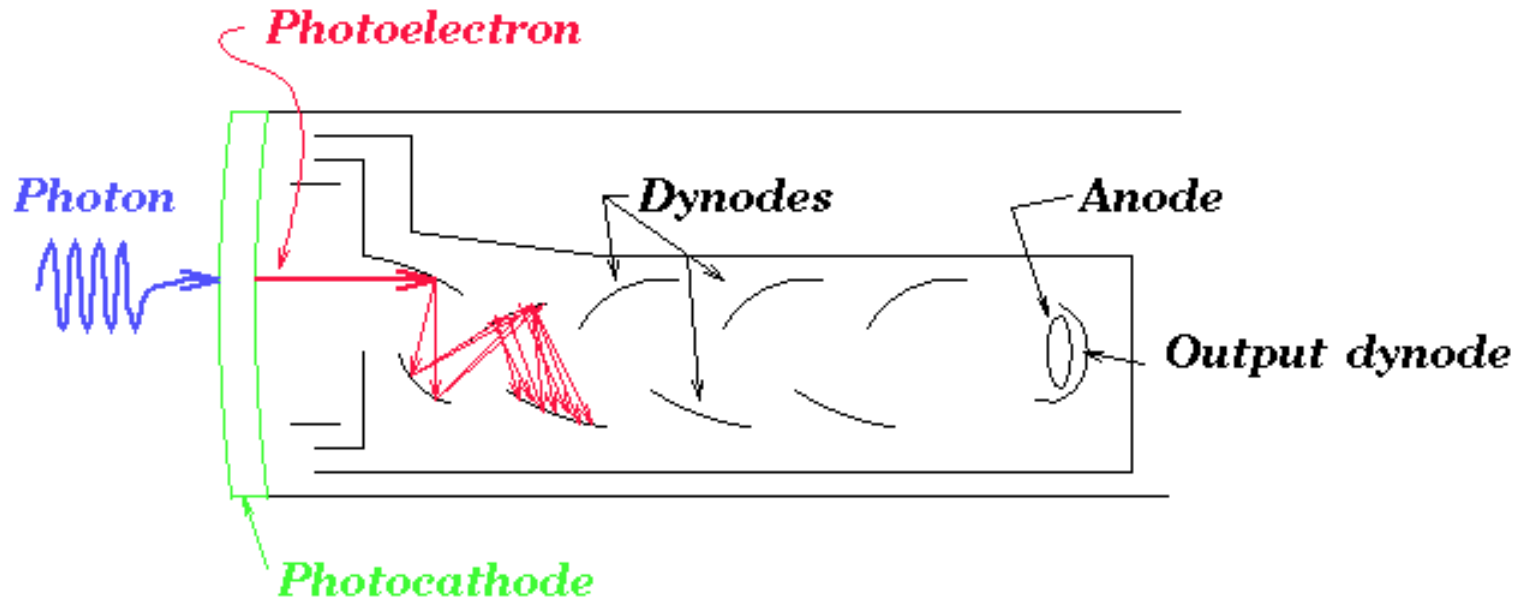


Thick scintillators are cheaper than thick semiconductors.

Energy resolution is worse because only part of optical light is collected.

Photomultipliers are the traditional photo-detectors.

Phototube



Photon produces an electron by interacting with photocathode.

Electron is accelerated by E-field, produces multiple electrons upon striking dynode. Several stages of dynodes can give multiplications of 10^6 . Response time is in nanoseconds.

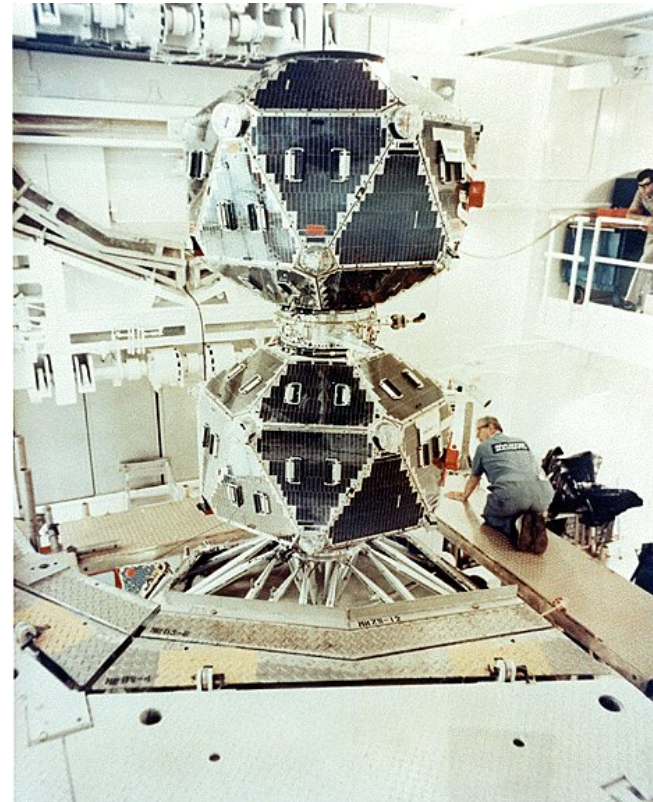
Discovery

Vela 5 a/b (launched in 1969) and Vela 6 a/b were each pairs on opposite sides of a circular orbit 250,000 kilometers in diameter.

Gamma-ray detector 60 cm³ of CsI. Events could be timed to an accuracy ~ 0.2 s, sometimes as good as 0.05 s.

The direction angle to the event with respect to the line between a pair of satellites could thus be determined to about 1/5th of a radian based on the difference in trigger times for the two satellites.

In 1973, Klebesadel, Strong, and Olsen published a paper describing 16 cosmic gamma-ray bursts observed in 1969-72.



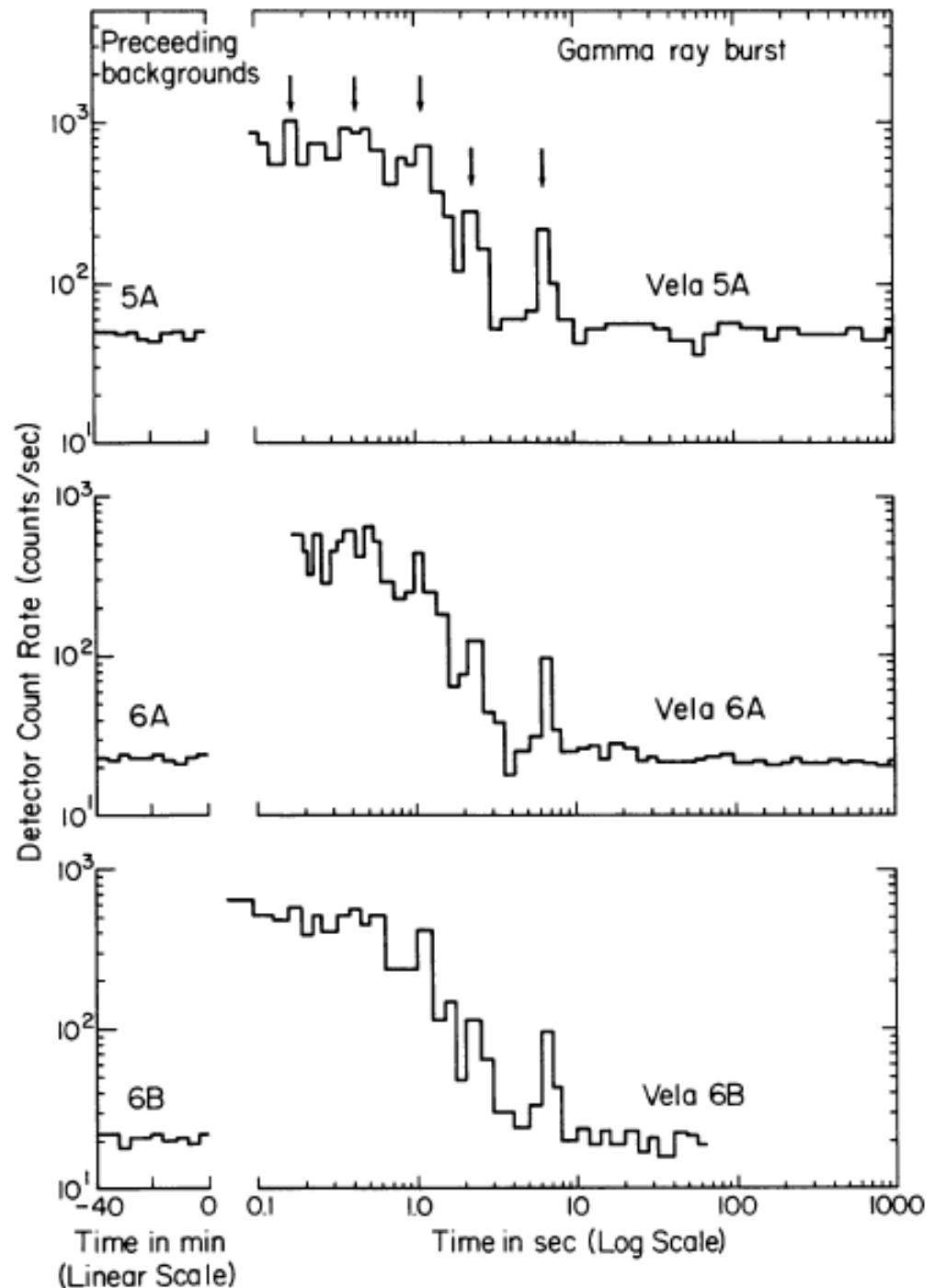
Discovery

1970 August 22 burst
from Klebesadel et al.
(1973).

Burst durations ranged
from 0.1 s to 30 s.

Burst fluences ranged
from 10^{-5} erg cm^{-2} to
 2×10^{-3} erg cm^{-2} .

Peak of spectrum above
10 keV maybe up to 10
MeV.



Interpretation of Early Bursts

Main question was Galactic or extra-Galactic.

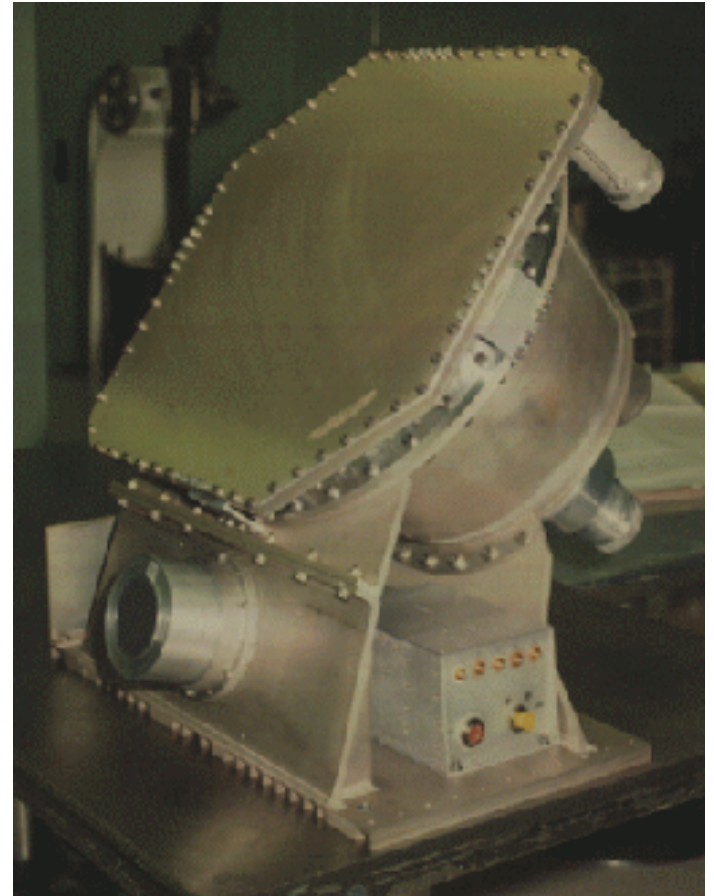
Galactic: distance ~ 10 kpc, total energy $\sim 10^{41} - 10^{43}$ erg

Extragalactic: distance ~ 10 Mpc, total energy $\sim 10^{47} - 10^{49}$ erg

BATSE

Large Area Detector - disk of NaI scintillation crystal 20 inches in diameter and 0.5 inch thick read out with three 5-inch PMTs. Quarter-inch plastic scintillation detector in front of the LAD for anticoincidence. Sensitive from 25 keV to 2 MeV.

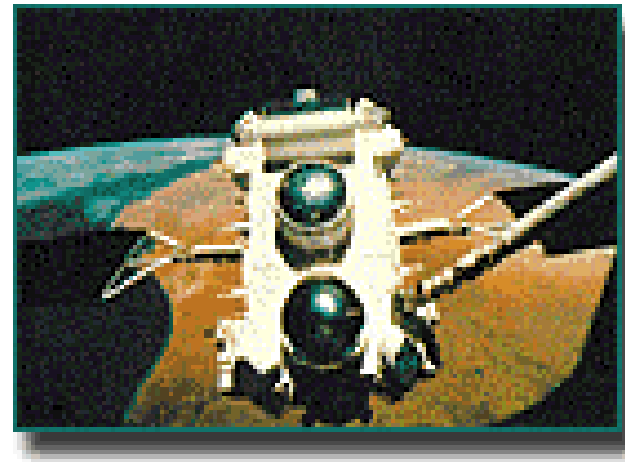
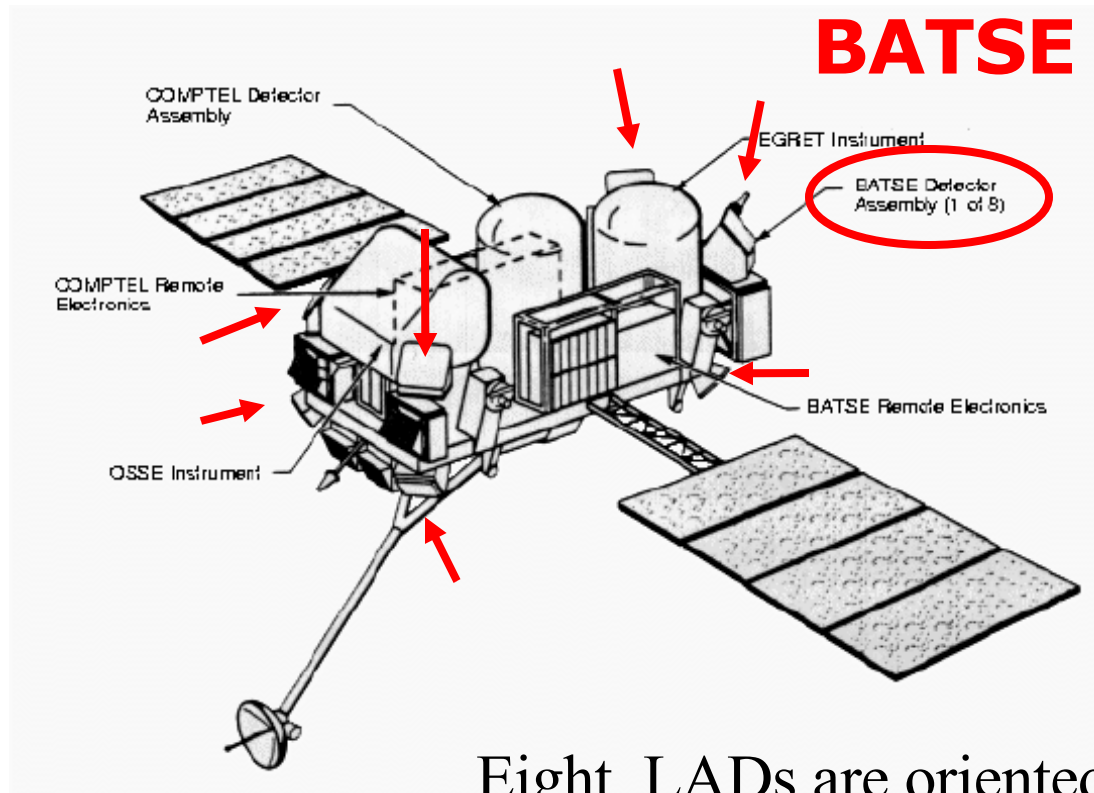
Spectroscopy Detector - NaI(Tl) 5 inches in diameter and 3 inches thick. Single 5 inch PMT.



BATSE



BATSE on CGRO



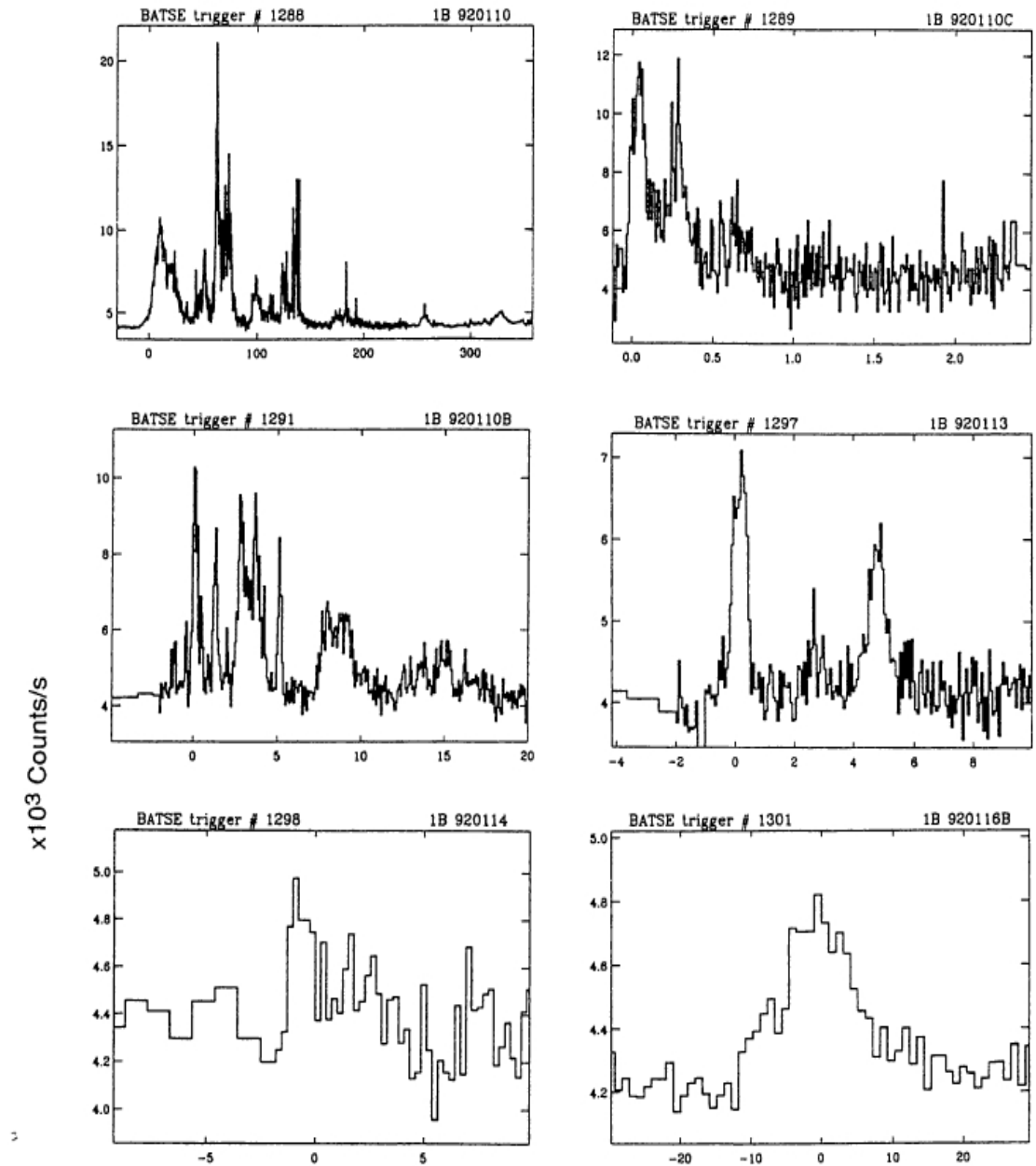
Eight LADs are oriented like the eight faces of an octahedron. Position of burst determined by relative counts in different detectors.

BATSE Bursts

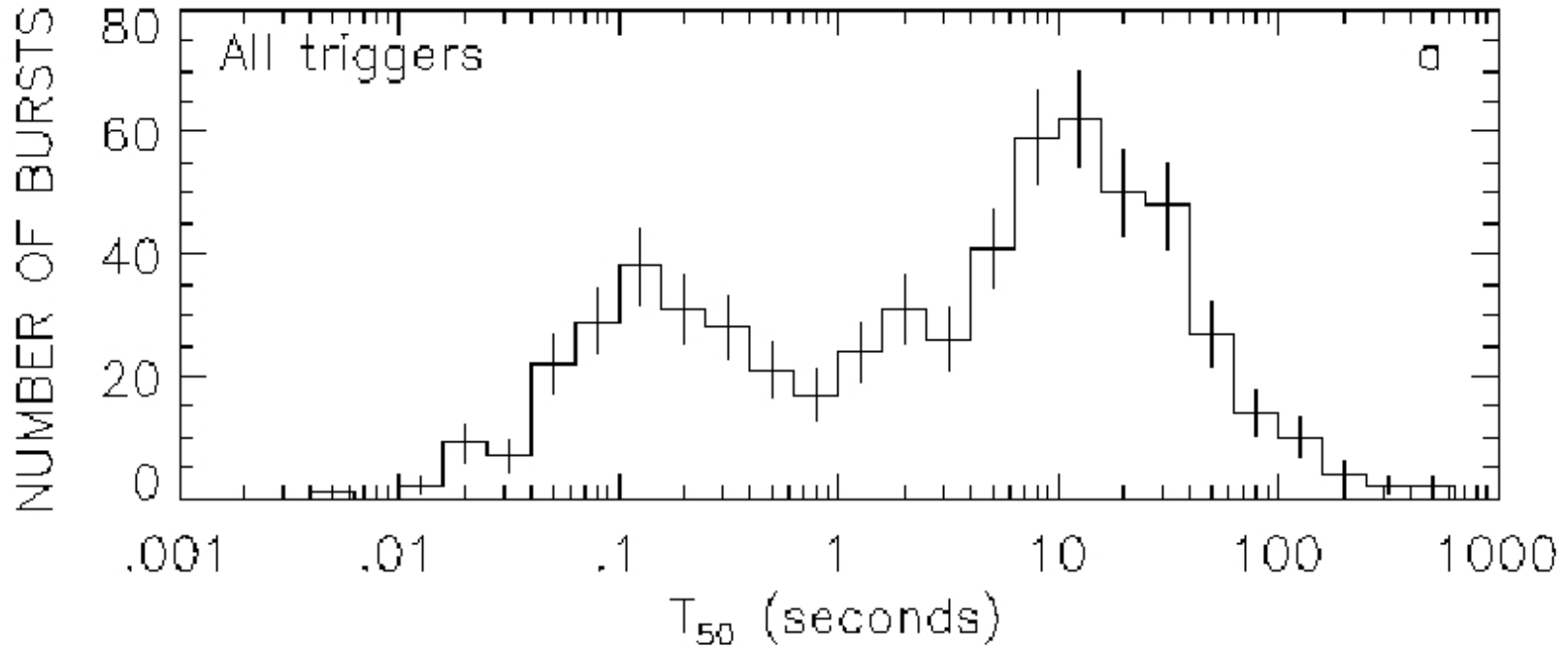
BATSE operated for 9 years and detected 2704 bursts.

Huge variety of GRBs varying on time scales from 10^{-3} to 10^3 seconds.

Bright bursts were localized to an accuracy of 2° dim ones to 10° . This prevented identifying X-ray or optical counterparts.



Long vs Short GRBs



Characterize burst durations by T_{50} and T_{90} . These are the minimum time intervals in which 50% or 90% of the burst fluence is contained.

GRB Spectra

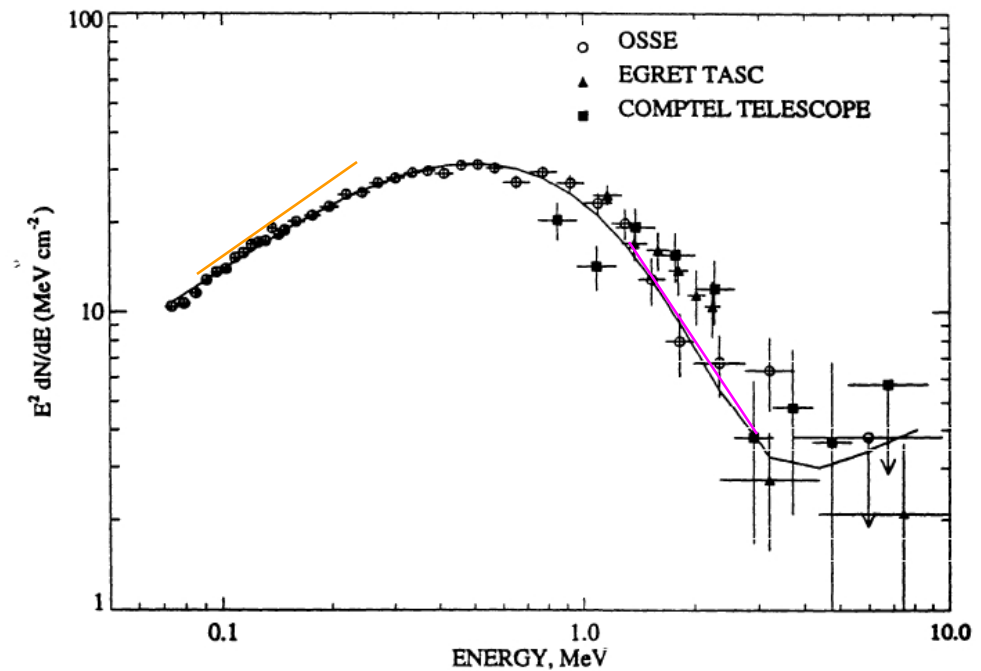


Figure 9 The spectrum of GB 910601 observed over a wide energy range, as measured by three experiments on *CGRO* (Share et al 1994). A typical broad spectrum with a peak power at about 600 keV is seen. (The fitted spectral up-turn above 4 MeV is not significant.)

PREECE ET AL.

BATSE SPECTROSCOPY CATALOG

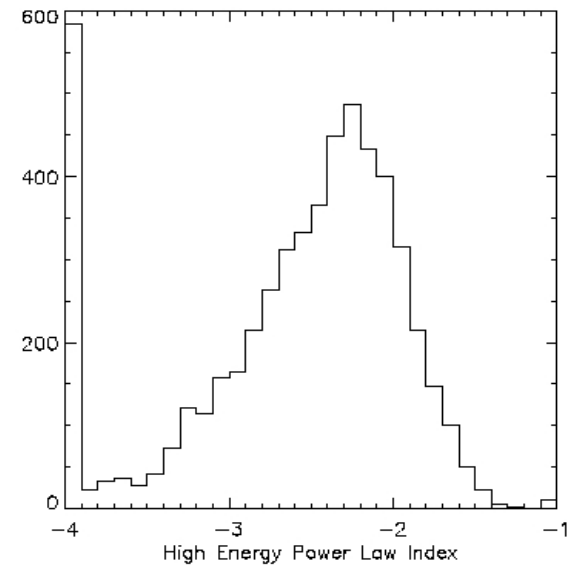
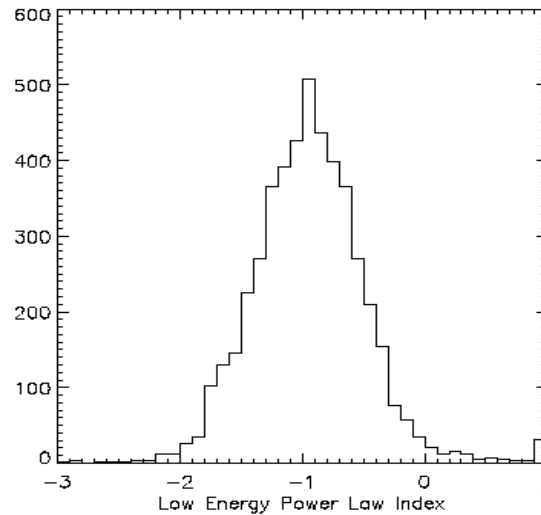
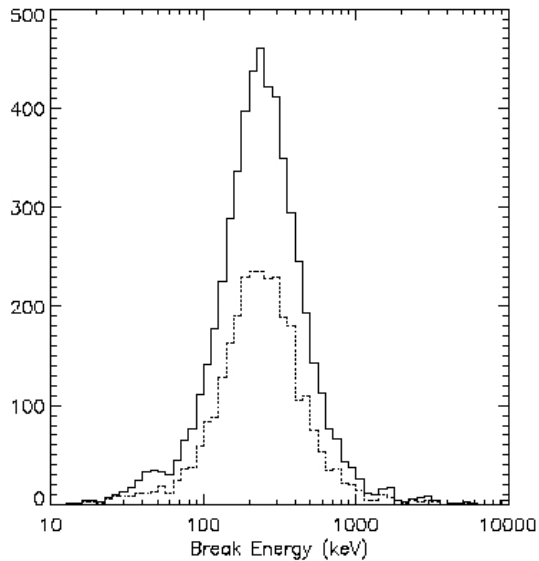
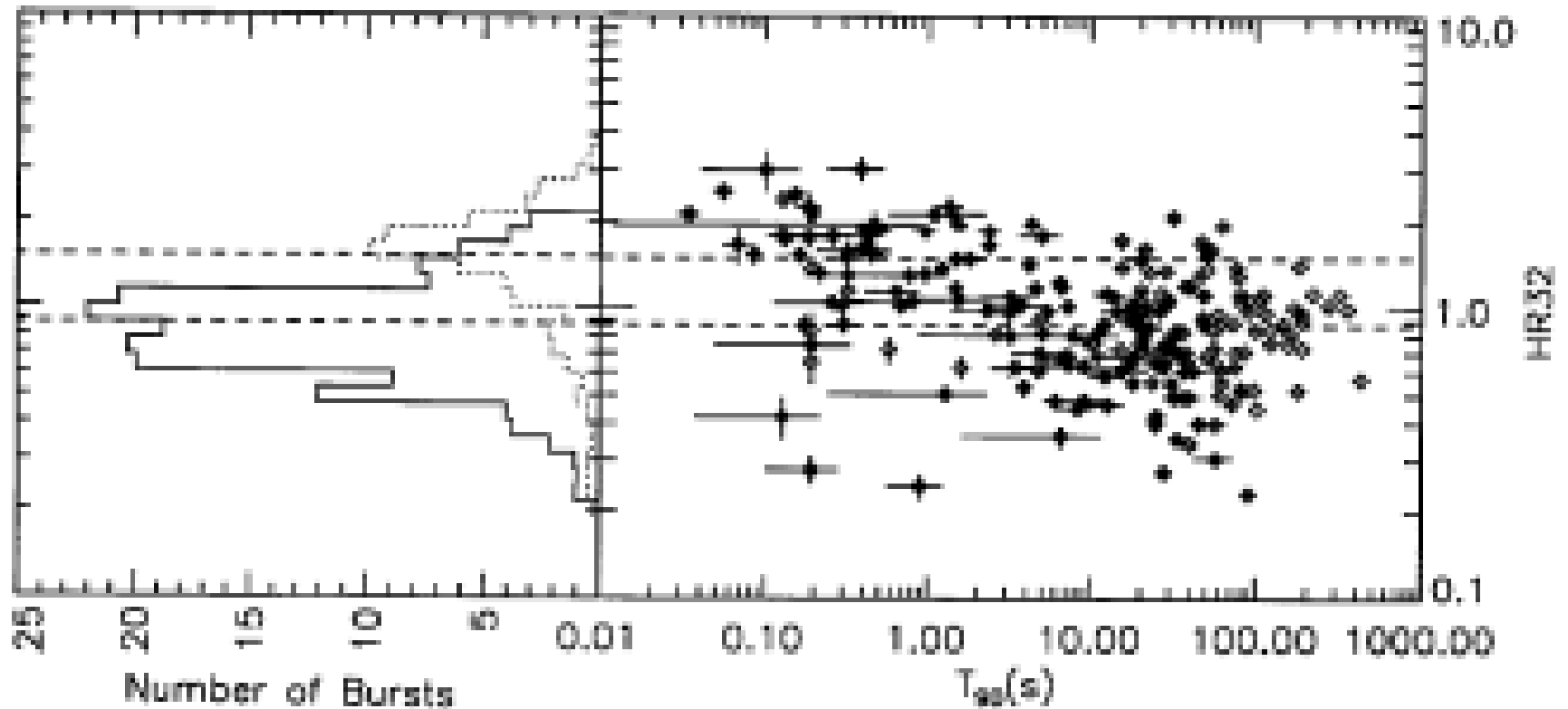


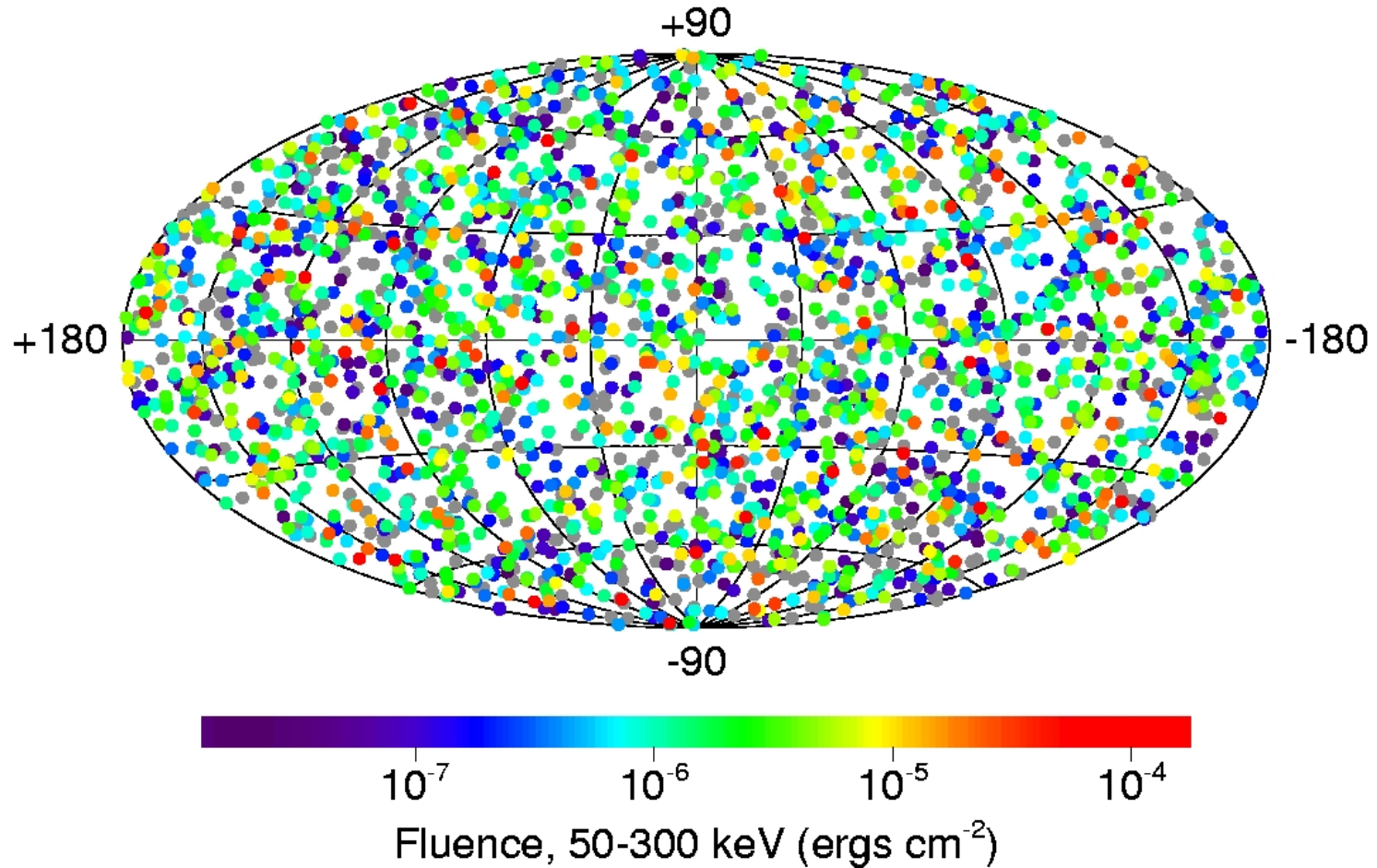
FIG. 7.—Low-energy power-law index distribution for the entire sample

Long vs Short GRBs



HR32 is ratio of counts in 100-300 keV band versus counts in 50-100 keV band. Short bursts appear to be harder than long ones.

2704 BATSE Gamma-Ray Bursts



First 153 bursts: $\langle \cos \theta \rangle = -0.002 \pm 0.006$, $\langle \sin^2 b \rangle = 0.310 \pm 0.006$

For isotropic: $\langle \cos \theta \rangle = 0.0$, $\langle \sin^2 b \rangle = 0.333$

Flux distribution

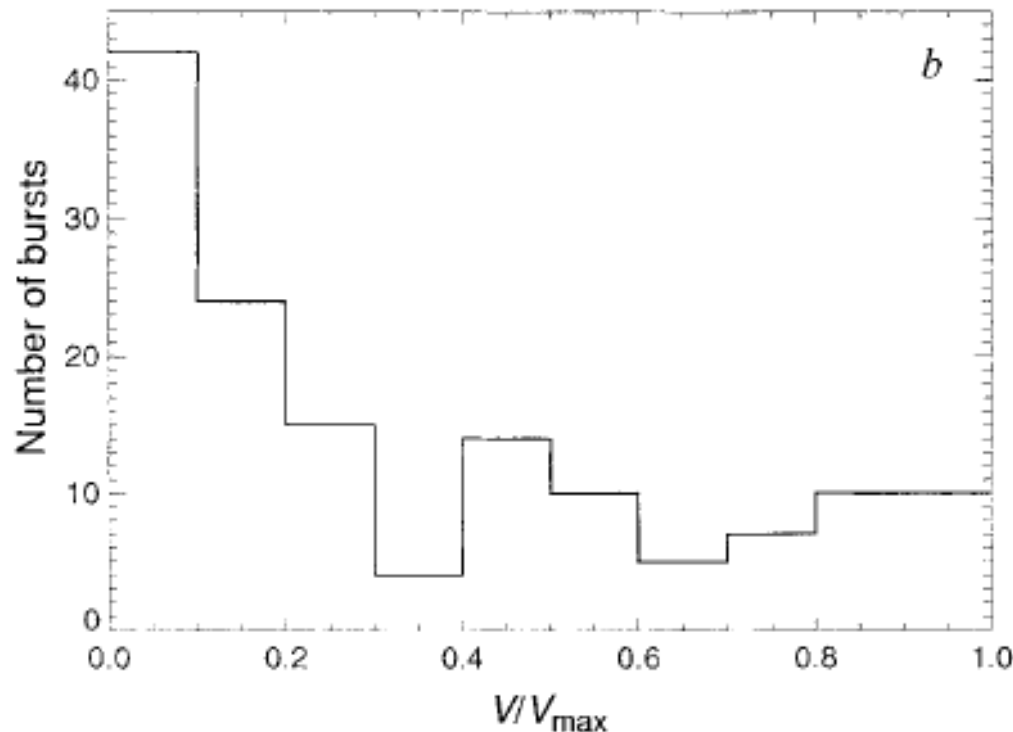
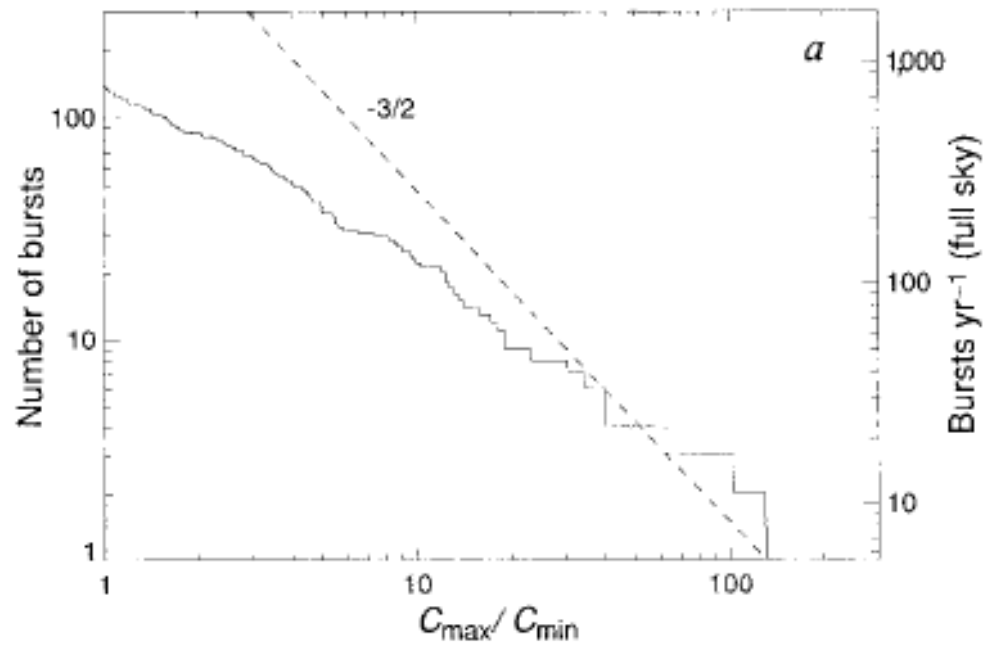
C_{\max} is burst maximum count rate, C_{\min} is trigger threshold.

$$V/V_{\max} = (C_{\max}/C_{\min})^{-3/2}$$

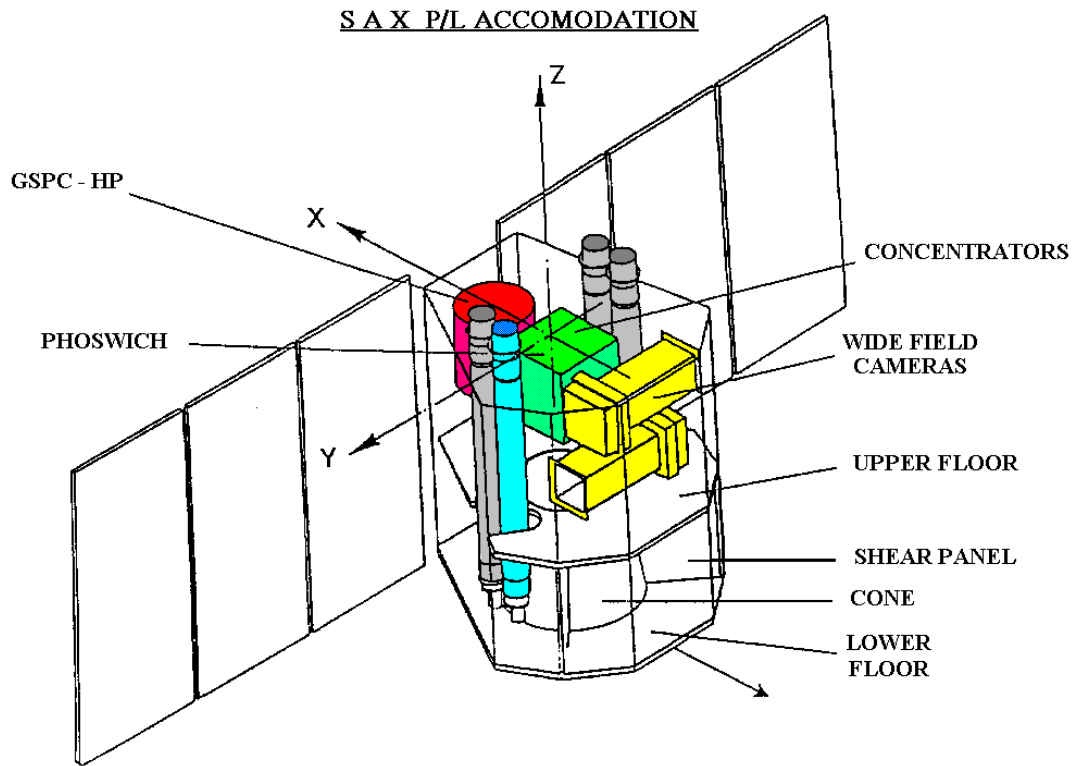
For homogeneous distribution, expect $\log(N>S)$ vs $\log(S)$ to follow $-3/2$ power law and $\langle V/V_{\max} \rangle = 0.5$.

Find $\langle V/V_{\max} \rangle = 0.35 \pm 0.02$ and deviations from $-3/2$ power law.

Conclude GRBs are isotropic, but not homogeneous.



BeppoSAX



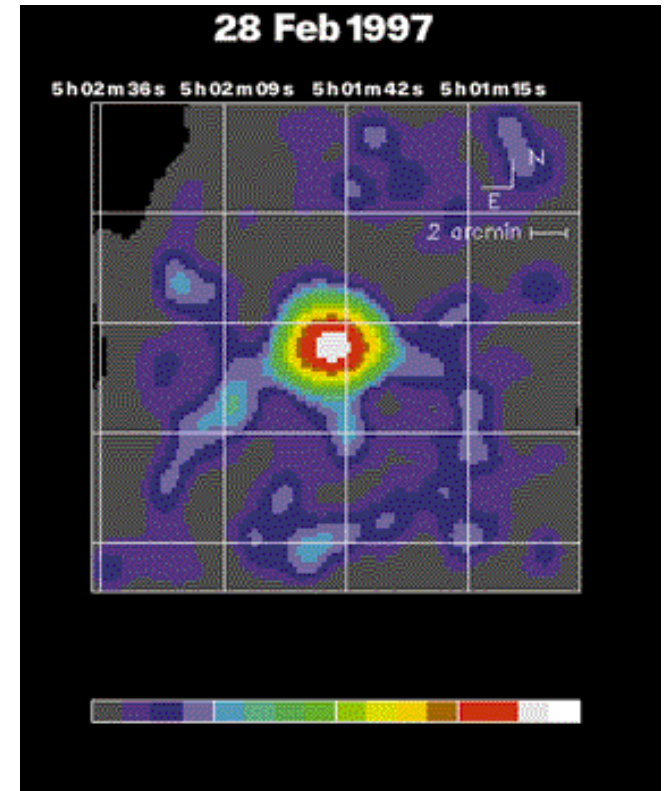
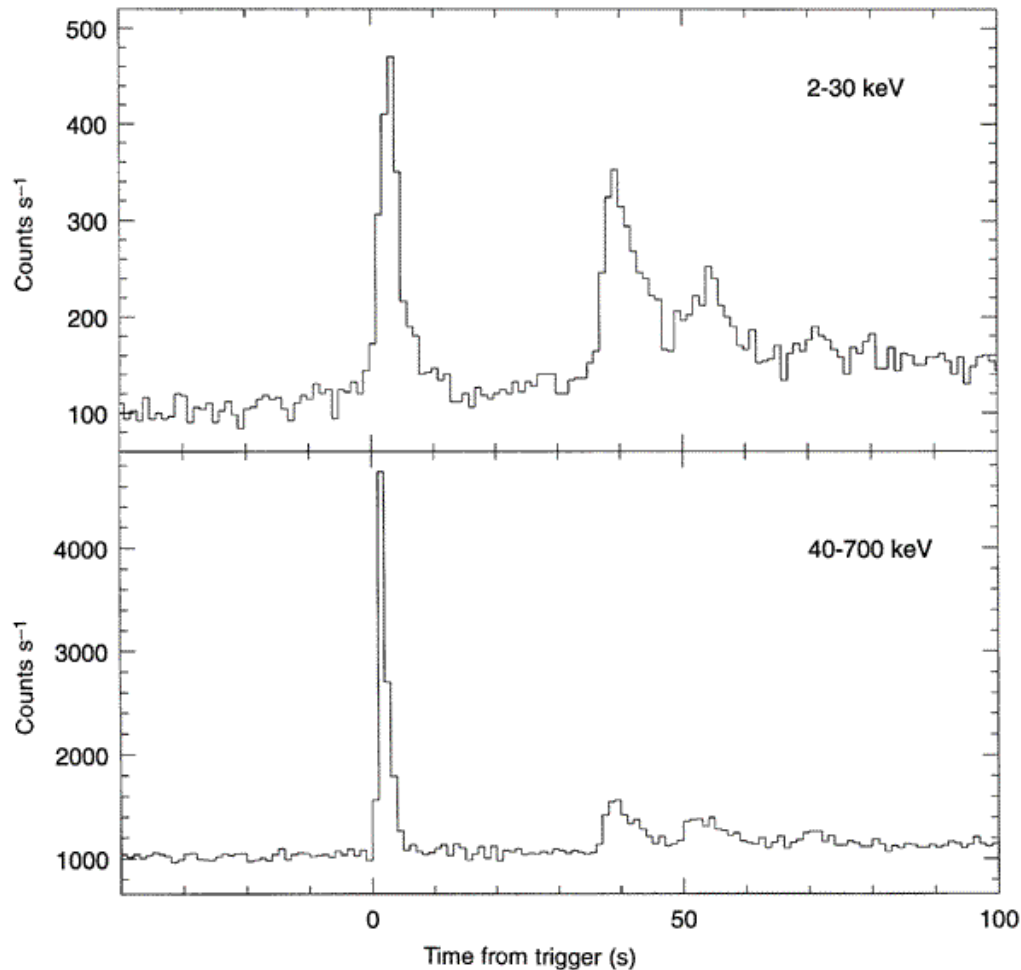
Italian-Dutch X-ray astronomy satellite.

Launched 1996.

Carried several X-ray instruments.

For GRBs, the critical instrument turned out to be the Wide Field Cameras: Proportional counters with effective area of 140 cm^2 and a coded aperture mask covering 2-30 keV with a field of view $20^\circ \times 20^\circ$.

First BeppoSAX WFC Burst

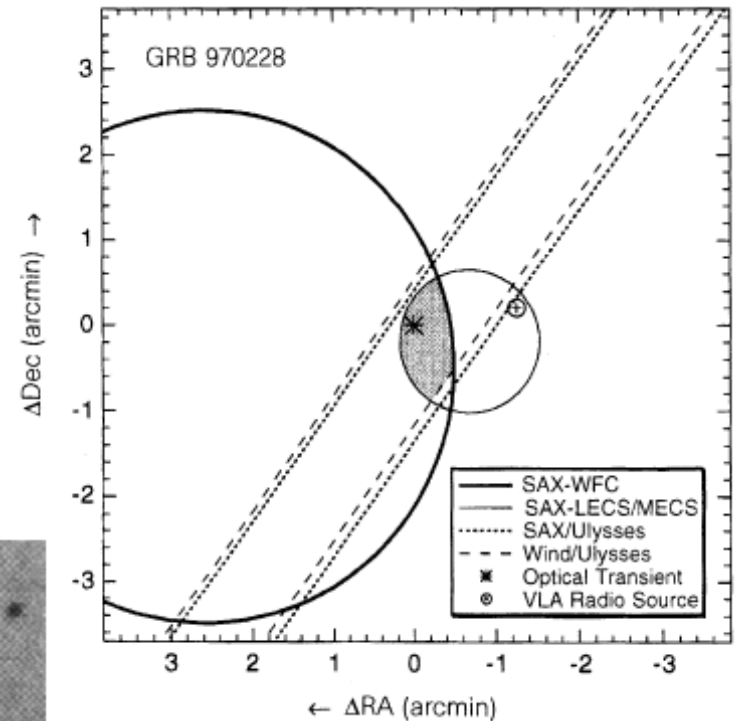
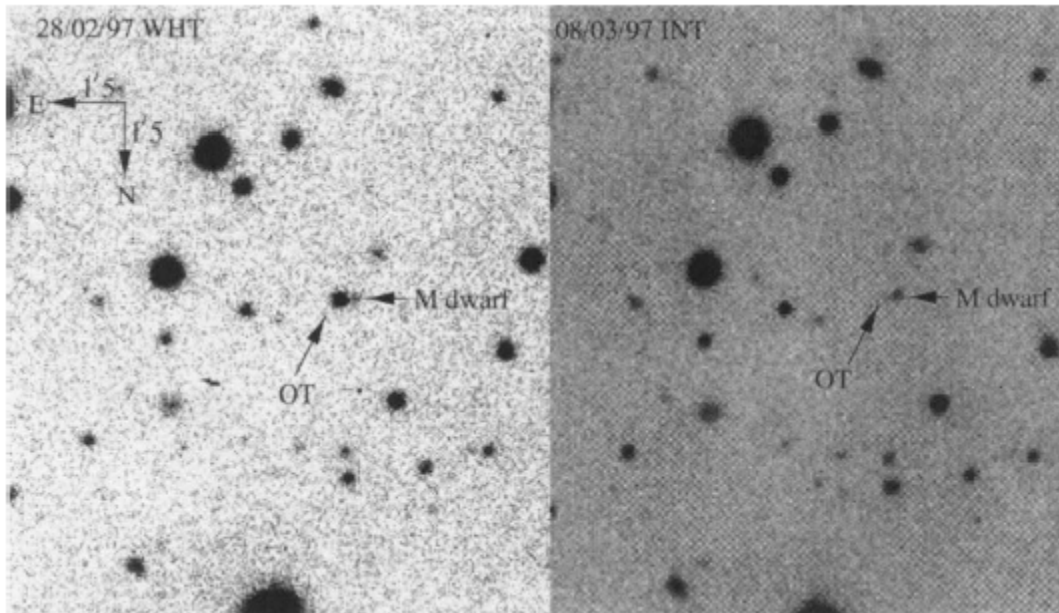


WFC light curve (top), GRB monitor light curve (bottom), narrow field instrument image (right) from Costa et al. 1997.

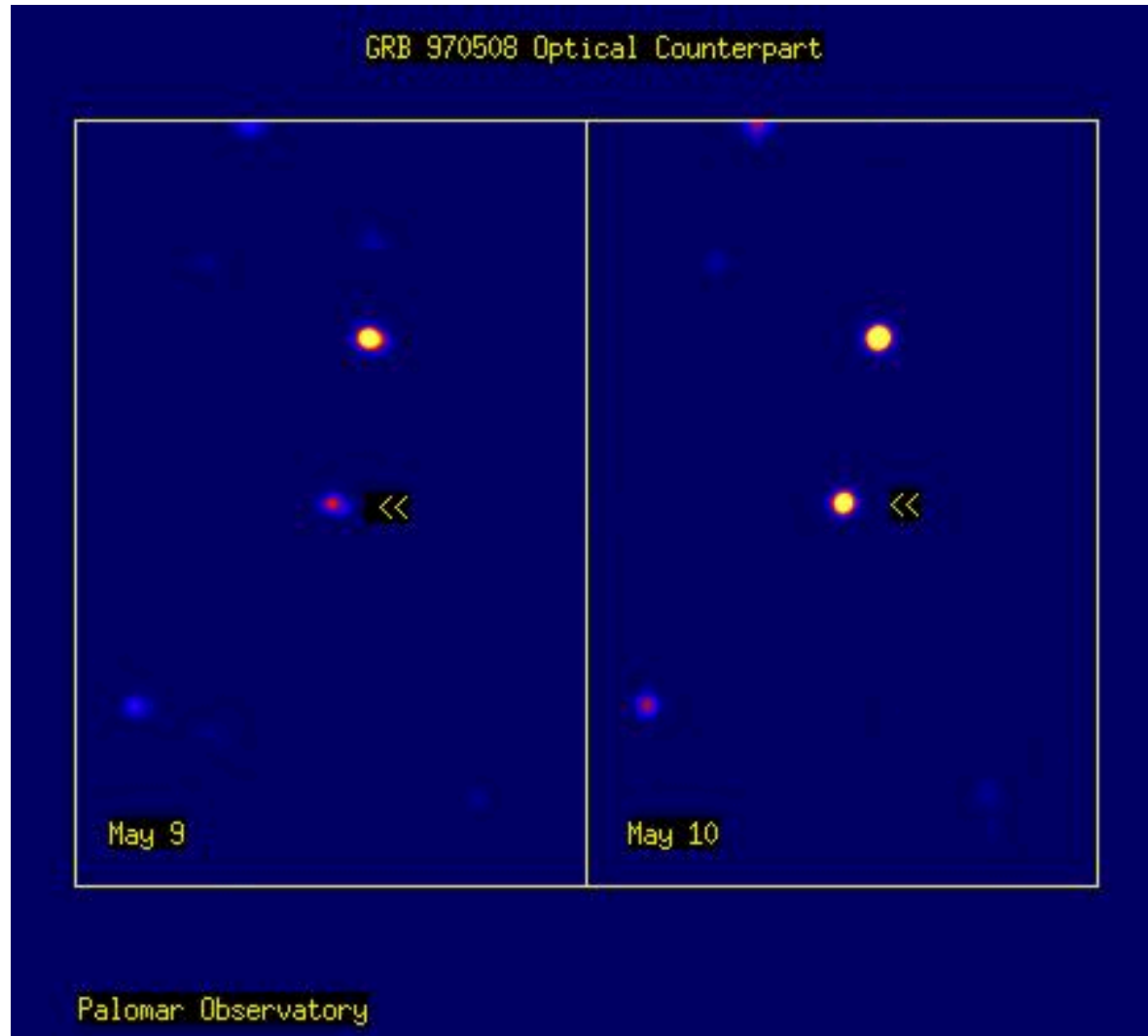
First GRB Optical Counterpart

Found decaying optical source inside BeppoSAX NFI error circle.

Found to lie near a faint and distant galaxy.

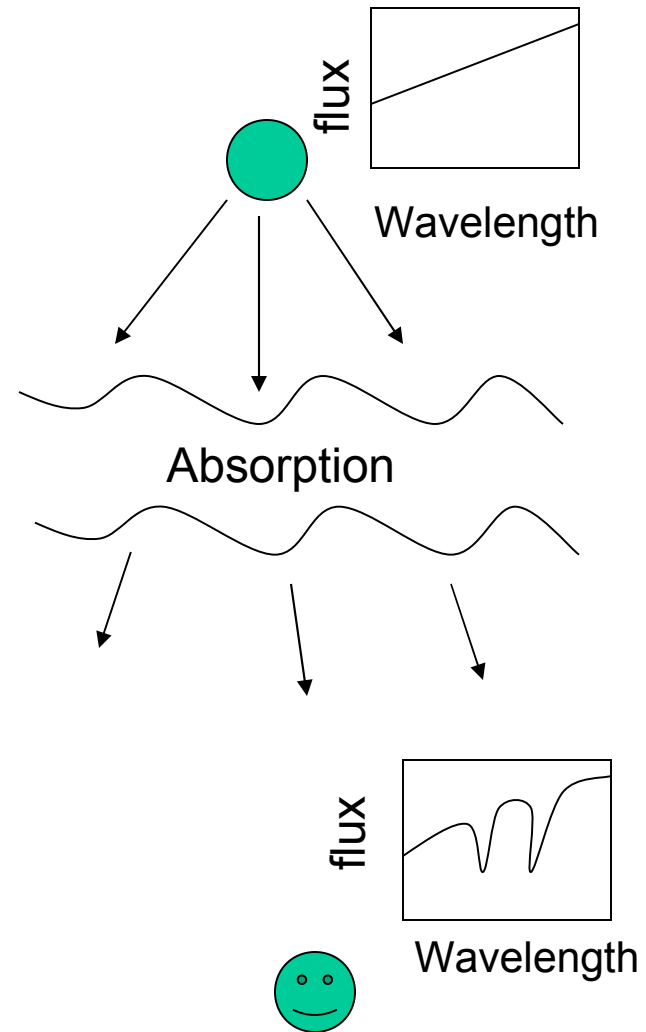
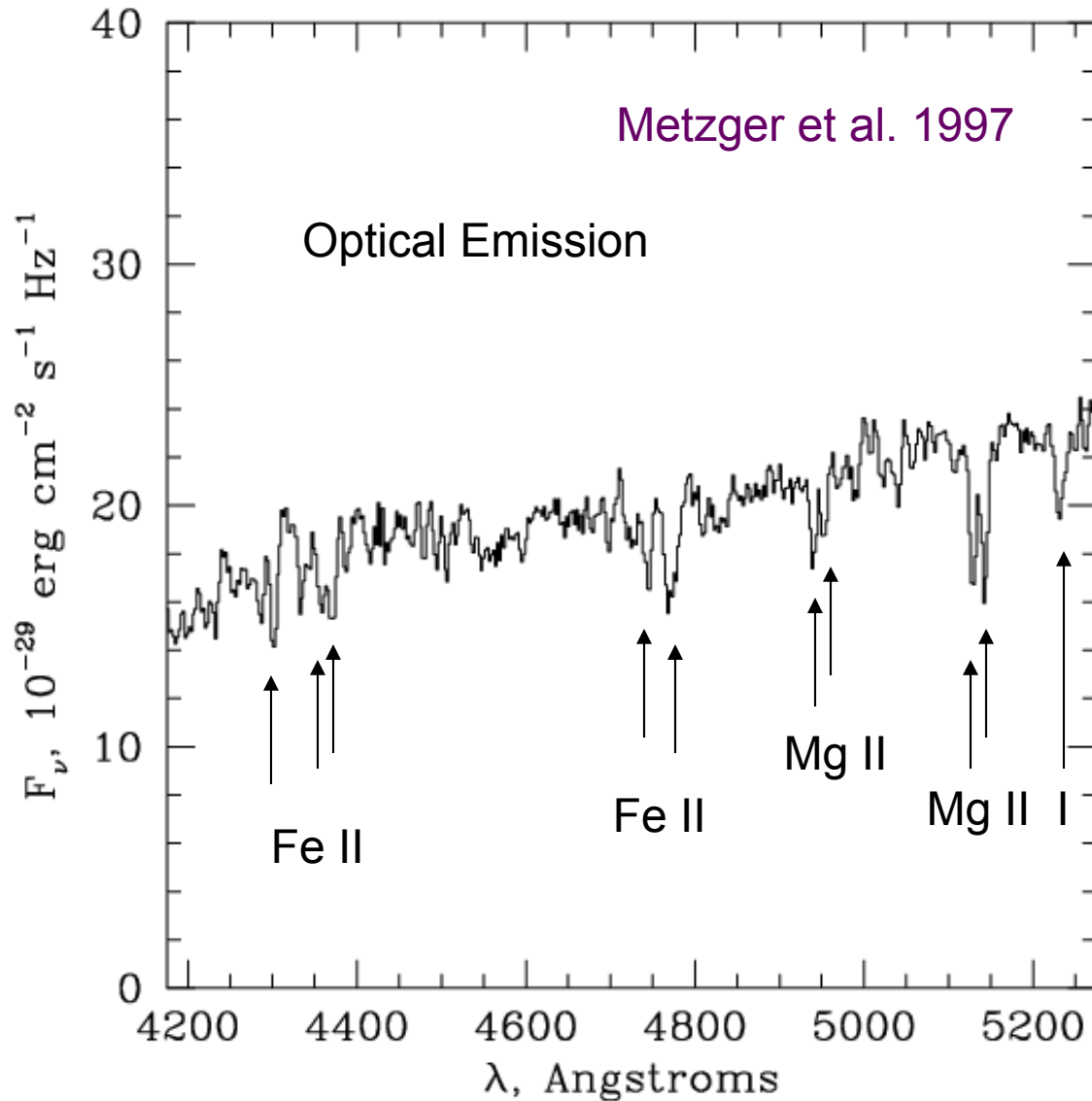


GRB 970508 – Optical Counterpart



BeppoSAX X-ray localization enabled detection of an optical transient. It was then possible to obtain an optical spectrum.

GRB970508 – Absorption Lines: $z=0.835$



Host Galaxy Detected for GRB970508

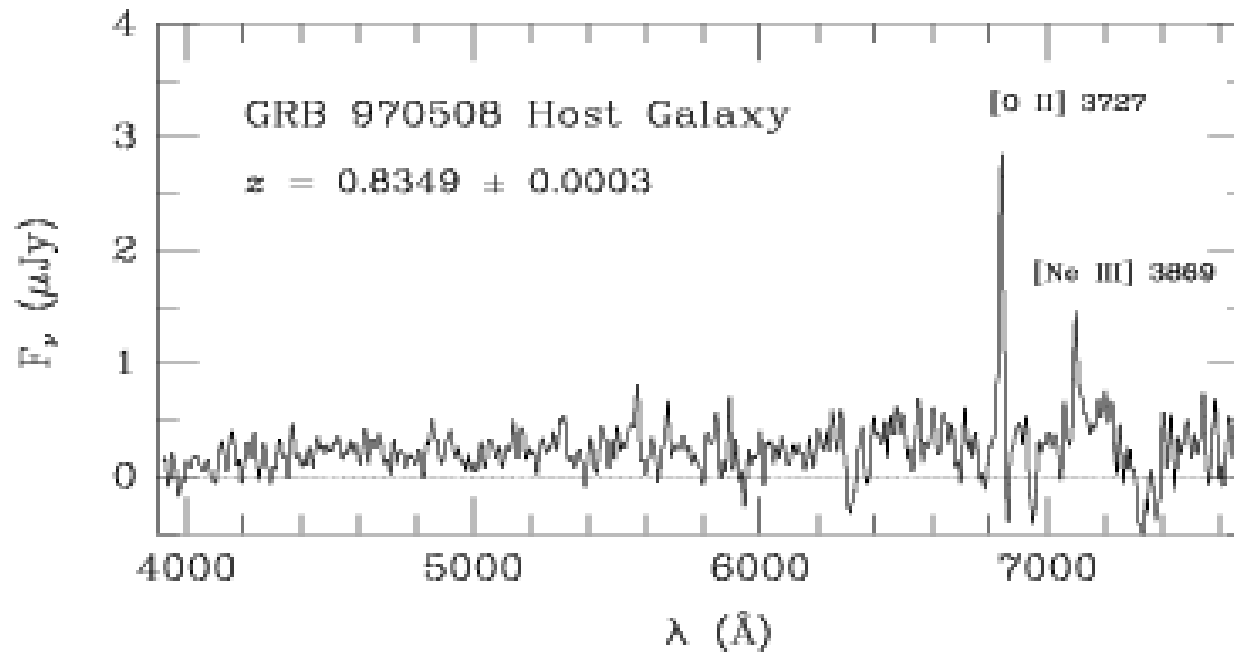


FIG. 2.— The weighted average spectrum of the host galaxy of GRB 970508, obtained at the Keck telescope. The spectra were smoothed with a Gaussian with a $\sigma = 5 \text{\AA}$, roughly corresponding to the instrumental resolution. Prominent emission lines are labeled.

PEAK PHOTON FLUXES AND ISOTROPIC LUMINOSITIES FOR GRBs WITH SECURE REDSHIFTS

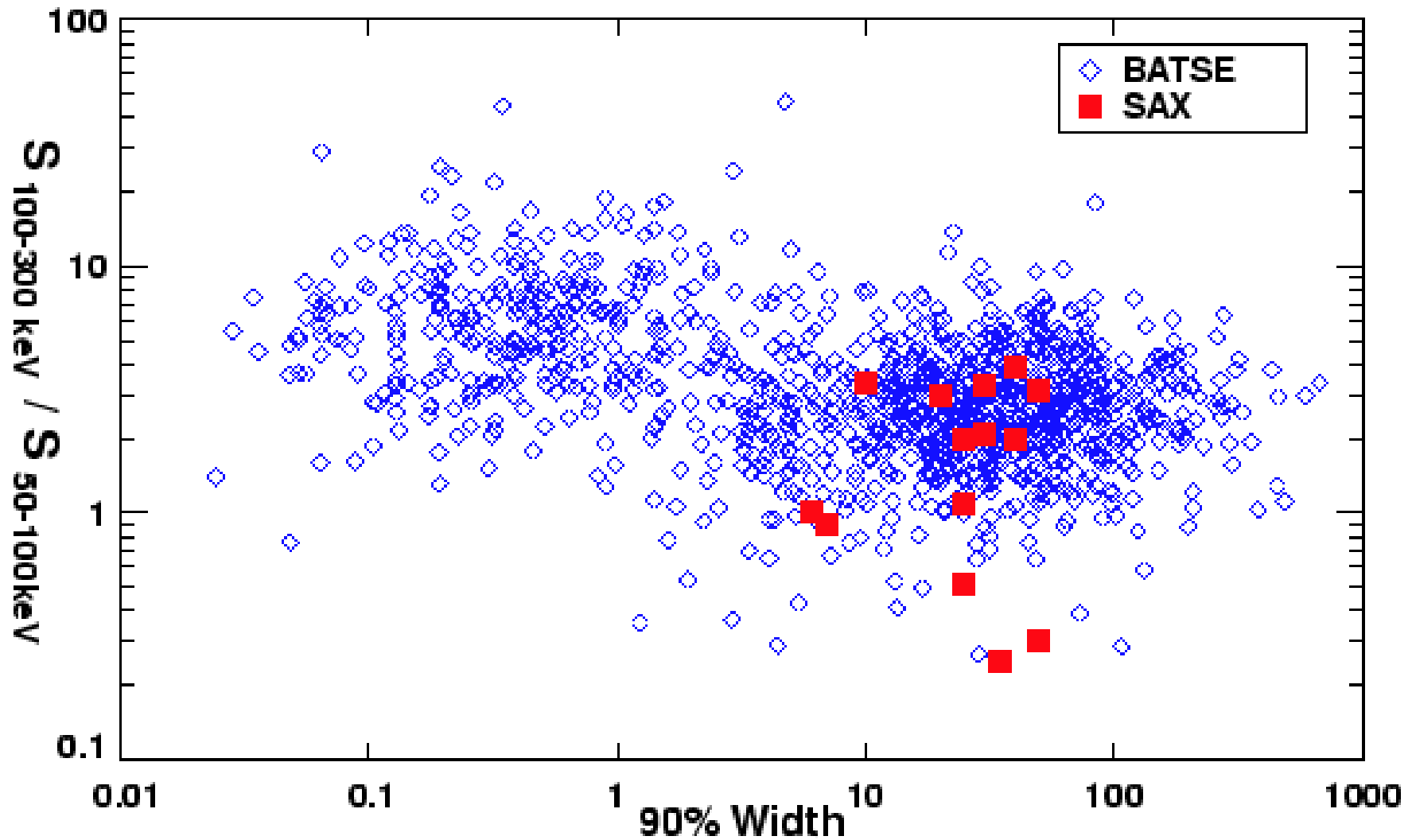
GRB	Redshift	P (photons $\text{cm}^{-2} \text{s}^{-1}$) ^a	L_P (photons s^{-1}) ^b	Redshift Reference
970228	0.695	3.5	5.1×10^{57}	1
970508	0.835	1.2	2.5×10^{57}	2, 3
971214	3.418	2.3	6.4×10^{58}	4
980613	1.096	0.63	2.3×10^{57}	5
980703	0.967	2.6	7.4×10^{57}	6
990123	1.600	16.4	1.2×10^{59}	7
990510	1.619	8.16	6.2×10^{58}	8
990712 ^c	0.430	9

Redshifts either measured for host galaxy after burst, or from absorption lines in optical after glow of the burst itself.

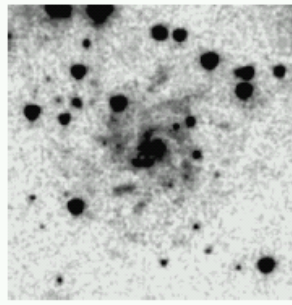
Clearly most bursts are at cosmological distances.

In BeppoSAX era, all bursts with afterglows and optical counterparts were long bursts.

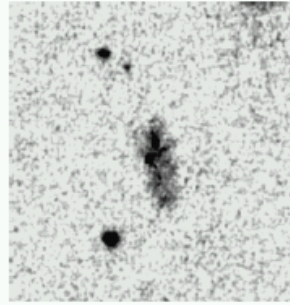
Long-duration GRBs are cosmological



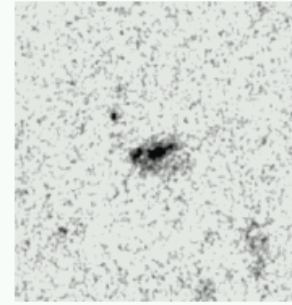
Host Galaxies



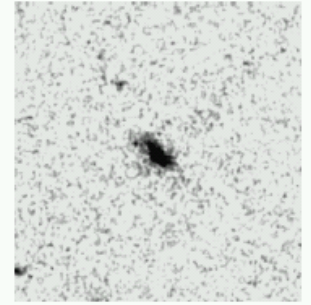
GRB 990705



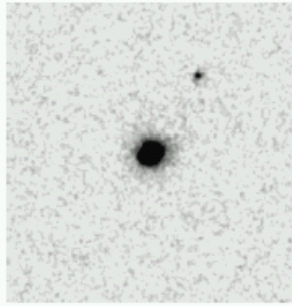
GRB 990506



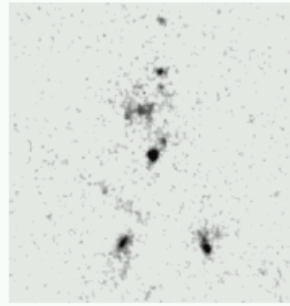
GRB 990123



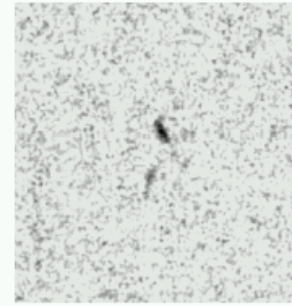
GRB 981226



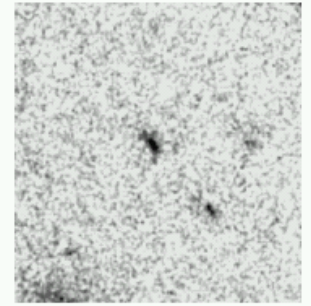
GRB 980703



GRB 980613



GRB 980519



GRB 971214

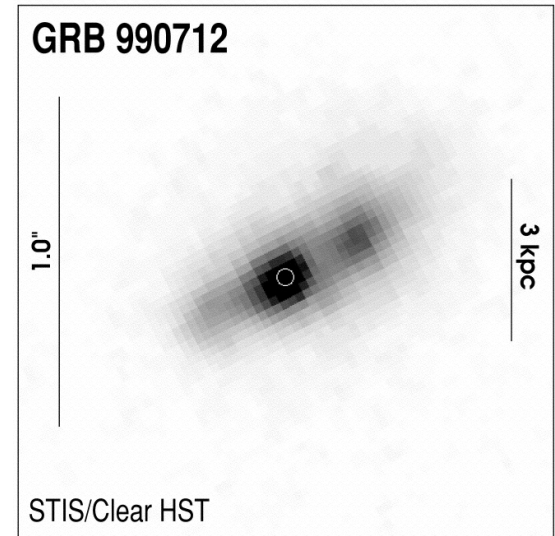
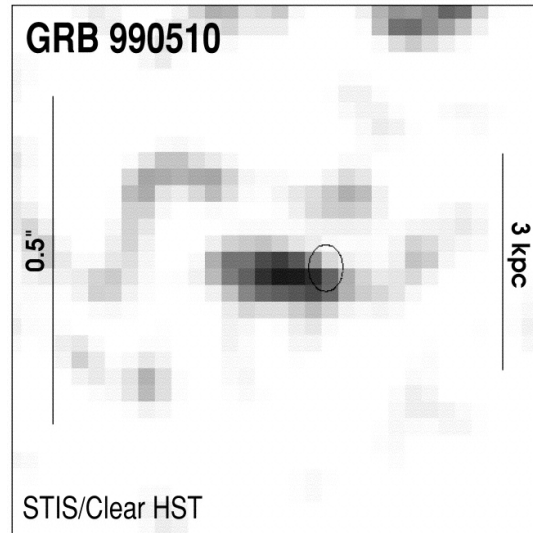
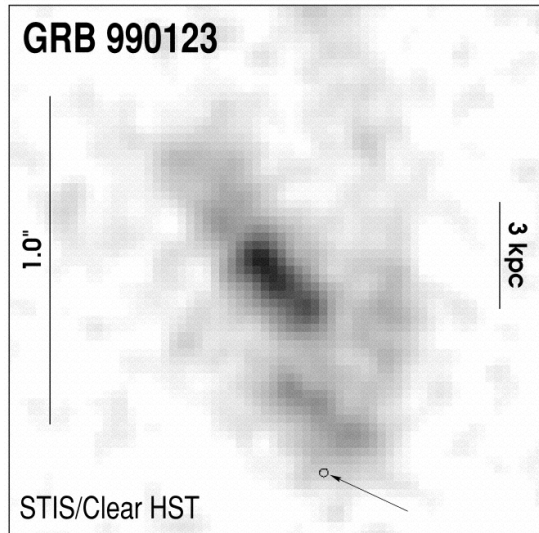
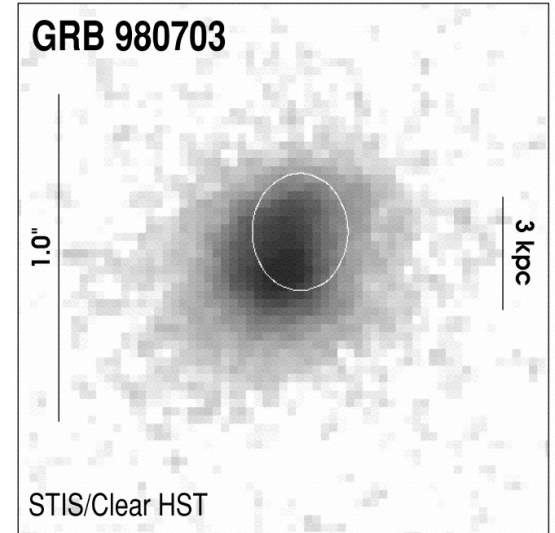
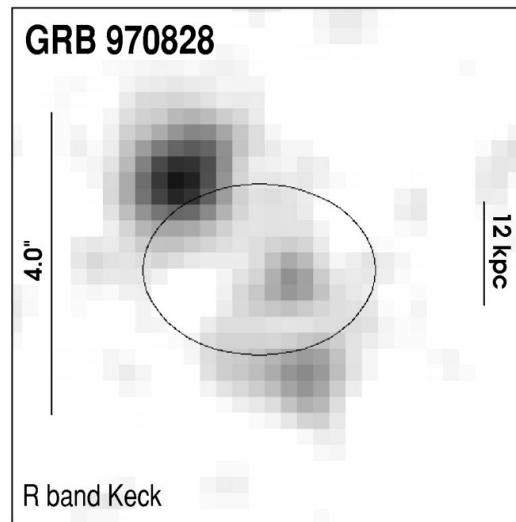
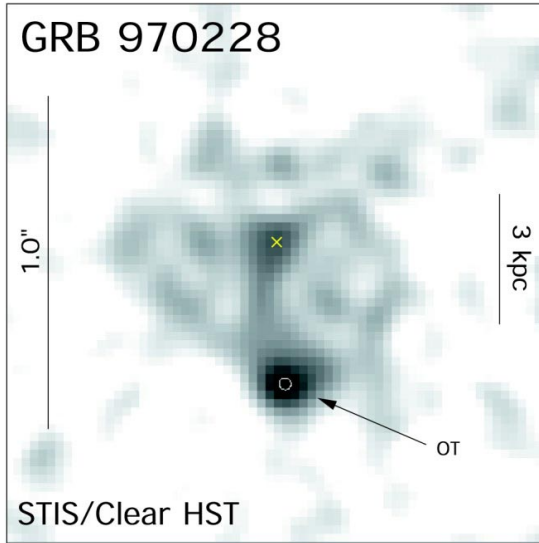
Holland 2001

TABLE 1. Specific star-formation rates for several GRB host galaxies.

GRB	z	R_{host}	$M_{\odot}\text{yr}^{-1}L_B^{*-1}$
970508	0.835	25.20	11.0
980613	1.096	24.56	20.0
980703	0.966	22.57	6.5
990123	1.600	24.07	11.0
990712	0.434	21.91	4.4

Hosts have high star formation rates and are generally similar to other star-forming galaxies at these redshifts.

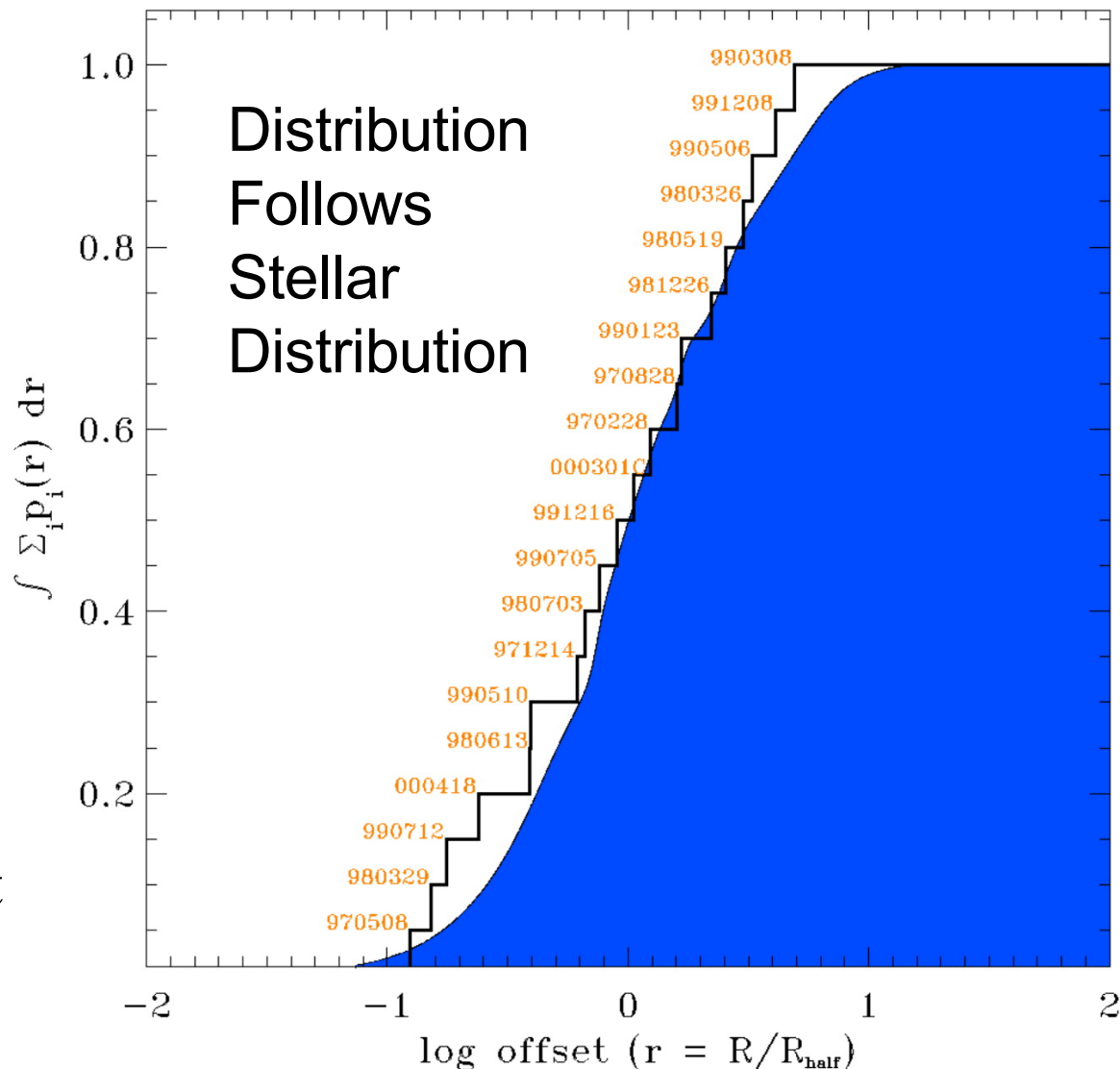
Location of GRB within Host



Location of GRB within Host

The environments of GRBs show higher gas densities, higher metallicities, and higher dust content than random locations in host galaxies.

Suggests that GRBs occur in star forming regions.



GRB Locations

- GRB hosts are star-forming galaxies
- GRBs trace the stellar distribution (in distance from galaxy center)
- GRBs occur in dense environments (probably star forming regions)
- Suggests long GRBs are associated with star formation and occur promptly after star formation

Connection of GRBs to Supernovae

SN 1998bw was found in the 8' error circle of GRB 980425 in observations made 2.5 days after the burst.

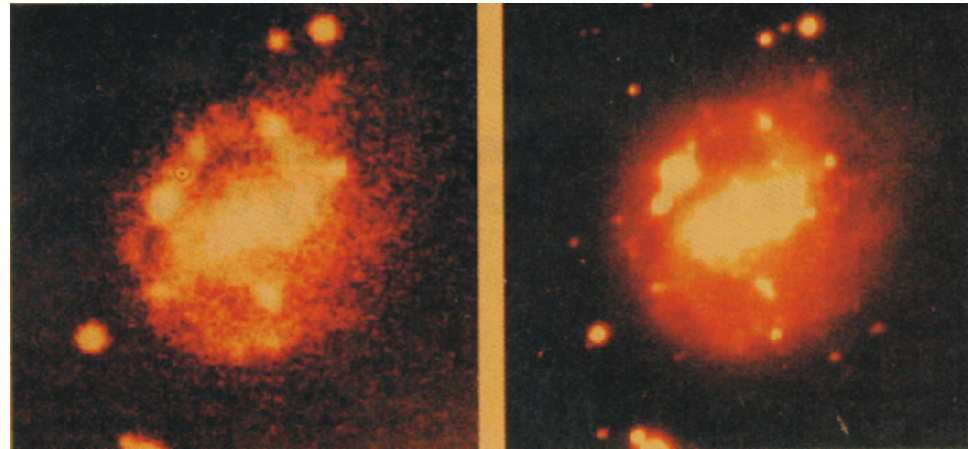
A slowly decaying X-ray source was subsequently found in the same galaxy ($z = 0.0085$) and identified with the GRB.

However, the GRB was very underluminous and the SN was very unusual with peculiar line emission (no H, no He, no Si at 615 nm).

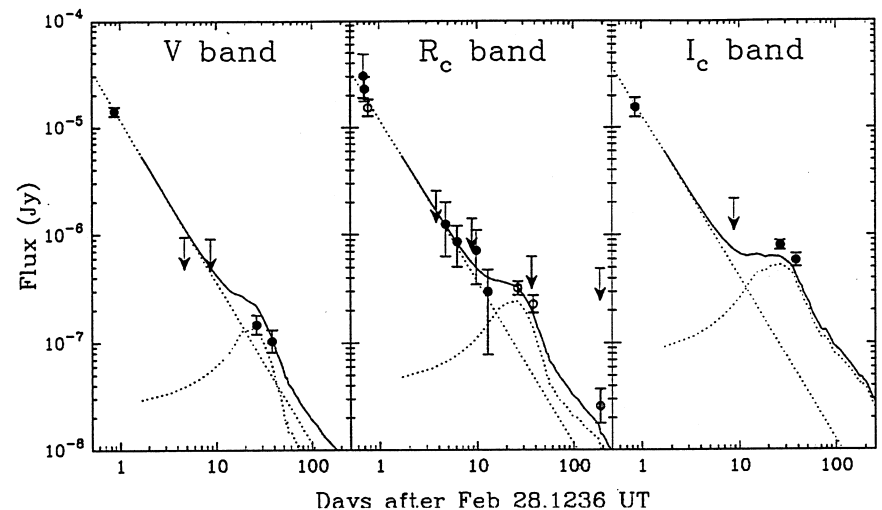
Radio emission a few days after GRB indicated relativistic outflow with energy $\sim 3 \times 10^{50}$ erg.

Thought to be oddball GRB and SN.

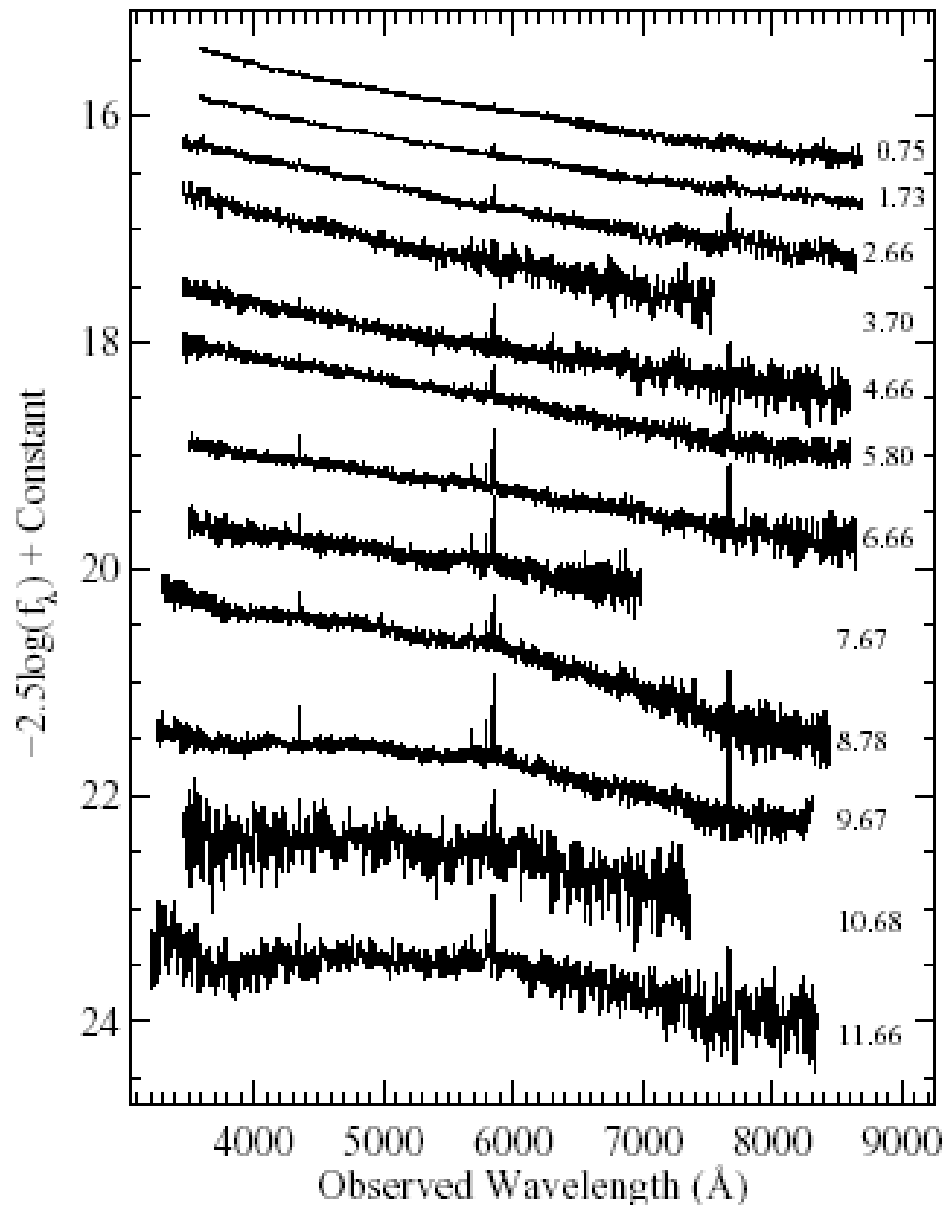
Host galaxy of SN 1998bw



light curves of GRB 970228



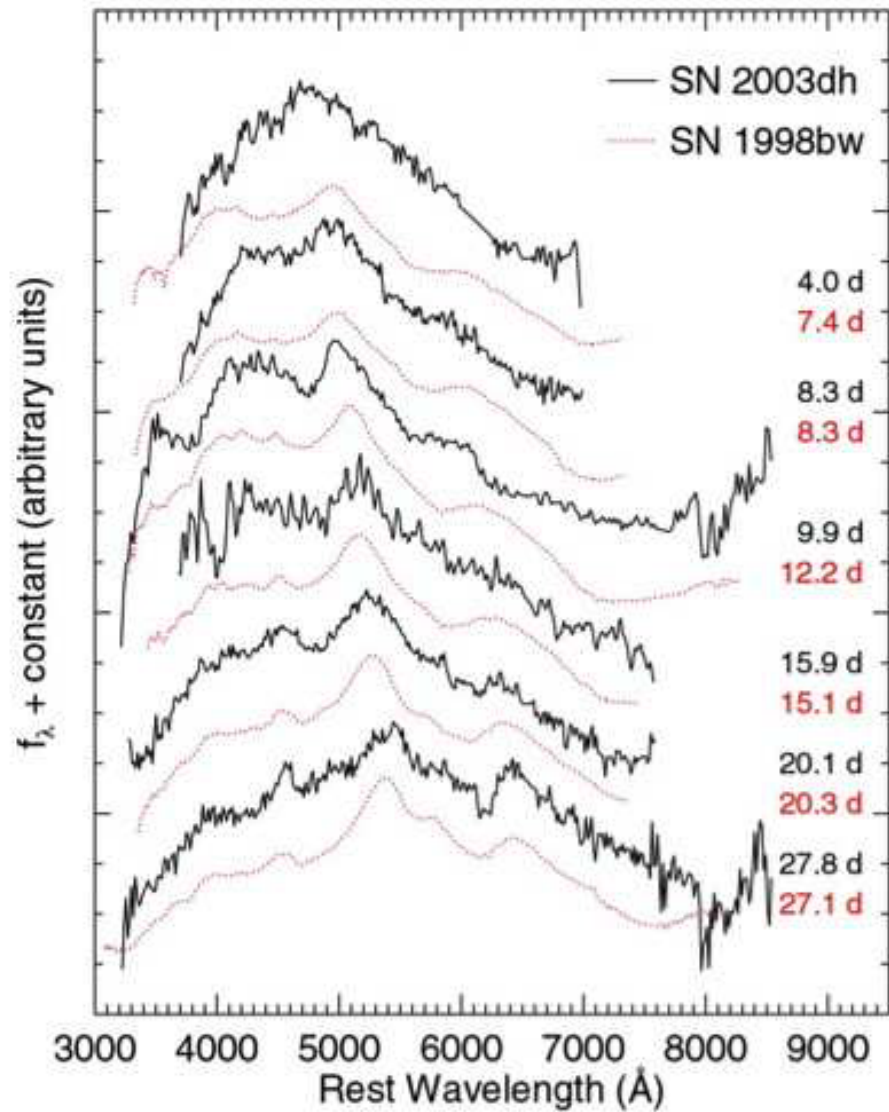
GRB030329 and SN 2003dh



Clear spectroscopic signature of a SN, broad emission lines, found after decay of afterglow of GRB030329.

“Smoking gun” linking GRBs and SNe.

SN 2003dh versus SN 1998bw



SN Bumps

light curves of GRB 970228

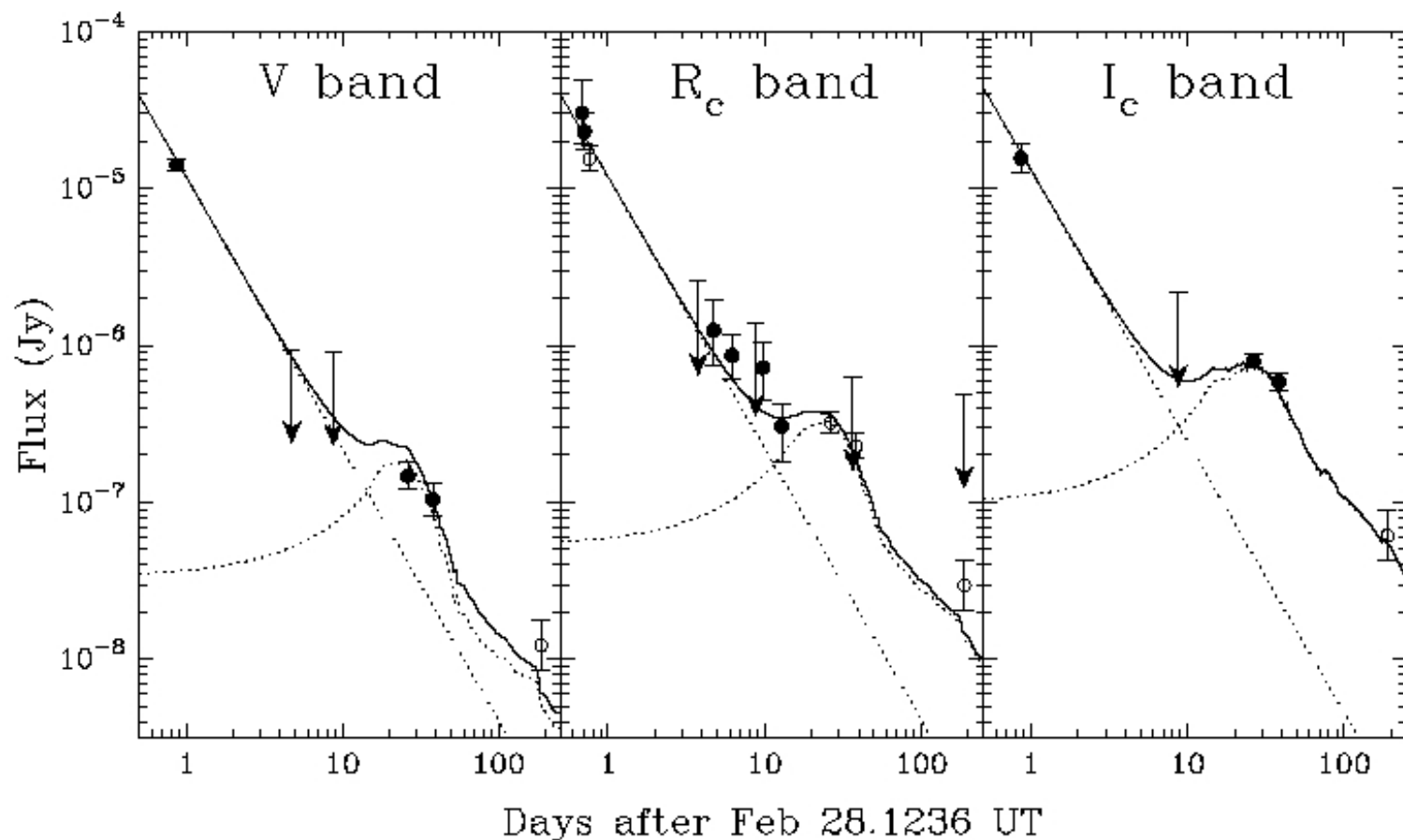


FIG. 3.— The V-, R_c-, and I_c-band lightcurves of GRB 970228 (fluxes versus time). The dotted curves indicate power-law decays with $\alpha = -1.73$, and redshifted SN 1998bw light curves. The thick line is the resulting sum of SN and power-law decay light curves.

GRB - Supernova

Name	z	Peak	T_{peak}^a	SN likeness/ designation
Burst/SN		[mag]	[day]	
GRB 980425/1998bw	0.0085	$M_V = -19.16 \pm 0.05$	17	Ic-BL
GRB 030329/2003dh	0.1685	$M_V = -18.8$ to -19.6	10 - 13	Ic-BL
GRB 031203/2003lw	0.1005	$M_V = -19.0$ to -19.7	18 - 25	Ibc-BL
XRF 020903	0.25	$M_V = -18.6 \pm 0.5$	~ 15	Ic-BL
GRB 011121/2001dk	0.365	$M_V = -18.5$ to -19.6	12 - 14	I (IIIn?)
GRB 050525a	0.606	$M_V \approx -18.8$	12	I
GRB 021211/2002lt	1.00	$M_V = -18.4$ to -19.2	~ 14	Ic
GRB 970228	0.695	$M_V \sim -19.2$	~ 17	I
XRR 041006	0.716	$M_V = -18.8$ to -19.5	16 - 20	I
XRR 040924	0.859	$M_V = -17.6$	~ 11	?
GRB 020405	0.695	$M_V \sim -18.7$	~ 17	I

Only a tiny fraction of SN are observed to be GRBs